The American Journal of Pathology, Vol. 183, No. 6, December 2013

ELSEVIER

The American Journal of PATHOLOGY

ajp.amjpathol.org

See related Commentary on page 1700

EPITHELIAL AND MESENCHYMAL CELL BIOLOGY

# TNF-α Modulation of Intestinal Epithelial Tight Junction Barrier Is Regulated by ERK1/2 Activation of Elk-1

Rana Al-Sadi,* Shuhong Guo,* Dongmei Ye,* and Thomas Y. Ma*†

*From the Department of Internal Medicine,* University of New Mexico School of Medicine, Albuquerque; and the Albuquerque Veterans Affairs Medical Center,† Albuquerque, New Mexico*

Accepted for publication September 3, 2013.

Address correspondence to Thomas Y. Ma, M.D., Ph.D., Internal Medicine-Gastroenterology, MSC105550, University of New Mexico, Albuquerque, NM 87131–0001. E-mail: tma@salud.unm.edu.

Tumor necrosis factor (TNF-α) is a proinflammatory cytokine that plays a critical role in the pathogenesis of inflammatory bowel disease. TNF-α causes an increase in intestinal permeability; however, the signaling pathways and the molecular mechanisms involved remain unclear. The major purpose of this study was to investigate the role of MAP kinase pathways (ERK1/2 and p38 kinase) and the molecular processes involved. An *in vitro* intestinal epithelial model system consisting of Caco-2 monolayers and an *in vivo* mouse model system were used to delineate the cellular and molecular mechanisms involved in TNF-α effects on tight junction barrier. The TNF-α–induced increase in Caco-2 tight junction permeability was mediated by activation of the ERK1/2 signaling pathway, but not the p38 kinase pathway. Activation of the ERK1/2 pathway led to phosphorylation and activation of the ETS domain-containing transcription factor Elk-1. The activated Elk-1 translocated to the nucleus, where it bound to its binding motif on the myosin light chain kinase (MLCK) promoter region, leading to the activation of *MLCK* promoter activity and gene transcription. In addition, *in vivo* intestinal perfusion studies also indicated that the TNF-α–induced increase in mouse intestinal permeability requires ERK1/2-dependent activation of Elk-1. These studies provide novel insight into the cellular and molecular processes that regulate the TNF-α–induced increase in intestinal epithelial tight junction permeability. *(Am J Pathol 2013, 183: 1871–1884; http://dx.doi.org/10.1016/j.ajpath.2013.09.001)*

Defective intestinal epithelial tight junction (TJ) barrier characterized by an increase in intestinal permeability is an important pathogenic factor contributing to the development of intestinal inflammation.[1–3] In various inflammatory diseases of the gut, including Crohn's disease, ulcerative colitis, celiac disease, and a number of infectious diarrheal syndromes, the disturbance in the intestinal TJ barrier allows increased antigenic penetration, contributing to the intestinal inflammatory response.[3–5] Tumor necrosis factor (TNF-α) is an essential mediator of inflammation in the gut.[6,7] TNF-α levels are markedly elevated in patients with inflammatory conditions of the gut.[8,9] It is well established that TNF-α causes an increase in intestinal TJ permeability *in vivo* and *in vitro*, which allows increased intestinal permeation of luminal antigens.[10–12] Animal studies have shown that enhancement of the intestinal TJ barrier prevents cytokine-mediated development of intestinal inflammation and diarrhea.[13,14] Clinical studies have shown that anti–TNF-α therapy leads to a retightening of the intestinal barrier and that the normalization of intestinal permeability is associated with long-term clinical remission.[7] In this regard, understanding the intracellular pathways and molecular mechanisms that mediate the TNF-α–induced increase in intestinal permeability is important for identifying potential therapeutic targets and developing therapeutic strategies to prevent disturbance of the intestinal TJ barrier and consequent antigenic penetration.

Previous studies from our research group and others have shown that TNF-α causes an increase intestinal epithelial TJ permeability[6,15–18] and indicated that myosin light chain kinase (MLCK) plays a central role in the TNF-α–induced increase in intestinal permeability.[6,17–19] TNF-α caused an increase in intestinal expression of MLCK, and inhibition of MLCK protein synthesis or MLCK activity prevented

Supported by a Veterans Affairs Merit Review grant from the Veterans Affairs Research Service and by NIH grants R01-DK064165 and R01-DK081429 (T.Y.M.).


http://dx.doi.org/10.1016/j.ajpath.2013.09.001

the TNF-α–induced increase in intestinal permeability. Furthermore, the increase in MLCK protein expression was directly related to up-regulation of *MLCK* gene activity and increase in mRNA transcription.[6,19] The targeted inhibition of MLCK and preservation of intestinal TJ barrier also resulted in inhibition of intestinal inflammation in various animal models of intestinal inflammation.[20,21] However, the intracellular signaling pathways and the precise molecular mechanisms that mediate TNF-α–induced activation of the *MLCK* gene and subsequent increase in intestinal permeability remain unclear. Mitogen-activated protein kinases (MAPK), including extracellular regulated protein kinase 1/2 (ERK1/2) and p38 kinase, have been suggested to play an important role in mediating proinflammatory actions of TNF-α, including cell growth, differentiation, stress, and inflammatory responses.[22–25] We hypothesized that TNF-α modulation of intestinal epithelial TJ permeability is mediated by MAPK pathway regulation of MLCK.

The major aims of the present studies were to investigate the intracellular signaling pathways and the molecular mechanisms that regulate TNF-α modulation of intestinal TJ permeability. We used both *in vitro* (filter-grown Caco-2 monolayers) and *in vivo* (live mouse intestinal perfusion) model systems to assess the intracellular and molecular mechanisms involved and to validate the *in vivo* relevance of the signaling and molecular pathways. We tested the hypothesis that the ERK1/2 or p38 kinase signaling pathway plays a key regulatory role in TNF-α–induced activation of *MLCK* and the subsequent increase in intestinal epithelial permeability. Our data suggest that the TNF-α–induced increase in intestinal TJ permeability is mediated by activation of the ERK1/2 signaling pathway, but not the p38 kinase pathway. Our data also suggest that ERK1/2 activation of nuclear transcription factor Elk-1 regulates *MLCK* gene activity by binding to the serum response element on the *MLCK* promoter region.

## Materials and Methods

### Chemicals

Cell culture media (Dulbecco's modified Eagle's medium), trypsin, fetal bovine serum, and related reagents were purchased from Life Technologies (Carlsbad, CA), as were glutamine, penicillin, streptomycin, and PBS. Anti–ERK1/2 (extracellular signal-regulated kinase 1/2), p-ERK1/2, Elk-1 (Ets-like gene 1), and p-Elk-1 antibodies were purchased from Abcam (Cambridge, MA). MLCK and anti–β-actin antibodies were purchased from Sigma-Aldrich (St. Louis, MO). Horseradish peroxidase–conjugated secondary antibodies for Western blot analysis were purchased from Life Technologies and Abcam (Cambridge, MA). siRNA of ERK1/2 and Elk-1 and transfection reagents were purchased from Dharmacon (Thermo Scientific, Pittsburgh, PA). The ERK1/2 inhibitor PD 98059 was purchased from Sigma-Aldrich. All other chemicals were purchased from Sigma-Aldrich, VWR International (West Chester, PA), Life Technologies, or Fisher Scientific.

### Cell Cultures

Caco-2 cells (passage 18 to 26) purchased from the ATCC (Manassas, VA) were maintained at 37°C in a 5% $CO_2$-enriched atmosphere, and they were kept in a culture medium composed of Dulbecco's modified Eagle's medium with 4.5 mg/mL glucose, 50 U/mL penicillin, 50 U/mL streptomycin, 4 mmol/L glutamine, 25 mmol/L HEPES, and 10% fetal bovine serum.

### Determination of Epithelial Monolayer Resistance and Paracellular Permeability

An epithelial voltohmmeter (World Precision Instruments, Sarasota, FL) was used for measurement of the transepithelial electrical resistance (TER) of filter-grown Caco-2 intestinal monolayers, as previously reported.[26,27] The effect of TNF-α on Caco-2 paracellular permeability was determined using an established paracellular marker, inulin, with a molar mass of 5000 g/mol.[26,28] For transepithelial and permeability studies, Caco-2–plated filters having TER of 400 to 500 $\Omega \cdot cm^2$ were used. A known concentration (2 μmol/L) of radiolabeled inulin ($^{14}C$) was added to the apical solution.

### Assessment of Protein Expression by Western Blot Analysis

Caco-2 monolayers were treated with 10 ng/mL TNF-α for varying time periods. At the end of the experimental period, Caco-2 monolayers were immediately rinsed with ice-cold PBS, and cells were lysed with lysis buffer [50 mmol/L Tris·HCl (pH 7.5), 150 mmol/L NaCl, 500 μmol/L NaF, 2 mmol/L EDTA, 100 μmol/L vanadate, 100 μmol/L phenylmethylsulfonyl fluoride, 1 μg/mL leupeptin, 1 μg/mL pepstatin A, 40 mmol/L paranitrophenyl phosphate, 1 μg/mL aprotinin, and 1% Triton X-100) and scraped, and the cell lysates were placed in microcentrifuge tubes. Cell lysates were centrifuged to yield a clear lysate. Supernatant was collected, and protein measurement was performed using a Bio-Rad protein assay kit (Bio-Rad Laboratories, Hercules, CA). Laemmli gel loading buffer was added to the lysate containing 20 μg of protein and boiled for 7 minutes, after which proteins were separated on SDS-PAGE gel. Proteins from the gel were transferred to a nitrocellulose membrane (Bio-Rad Laboratories) overnight. The membrane was incubated for 2 hours in blocking solution (5% nonfat dried milk in Tris-buffered saline–Tween 20 buffer). The membrane was incubated with appropriate primary antibodies in blocking solution. Primary antibodies were used in concentrations according to the manufacturer's recommendations (usually 1 to 2 μg/mL). After being washed in Tris-buffered saline–1% Tween buffer, the membrane was incubated in appropriate secondary antibodies (1:2000). After a washing in Tris-buffered saline–1% Tween 20 buffer, the membrane was developed using Luminol Western blotting reagents (Santa

Cruz Biotechnology, Santa Cruz, CA) on Kodak BioMax MS film (Fisher Scientific).

### RNA Isolation and Reverse Transcription

Caco-2 cells ($5 \times 10^5$/filter) were seeded into six-well Transwell permeable inserts (Corning Life Sciences, Tewksbury, MA) and grown to confluency. Filter-grown Caco-2 cells were then treated with the appropriate experimental reagents for the desired time periods. At the end of the experimental period, cells were washed twice with ice-cold PBS. Total RNA was isolated using an RNeasy kit (Qiagen, Valencia, CA) according to the manufacturer's protocol. Total RNA concentration was determined by absorbance at 260/280 nm using a SpectraMax 190 microplate reader (Molecular Devices, Sunnyvale, CA). The reverse transcription was performed using an Applied Biosystems GeneAmp Gold RNA PCR core kit (Life Technologies). From each sample, 2 μg of total RNA was reverse-transcribed into cDNA in a 40-μL reaction containing 1× RT-PCR buffer, 2.5 mmol/L $MgCl_2$, 250 μmol/L of each dNTP, 20 U RNase inhibitor, 10 mmol/L dithiothreitol, 1.25 μmol/L random hexamer, and 30 U MultiScribe Reverse Transcriptase. The reverse-transcriptase reactions were performed in a thermocycler (PTC-100; MJ Research, Waltham, MA) at 25°C for 10 minutes, 42°C for 30 minutes, and 95°C for 5 minutes.

### qPCR Quantification of Gene Expression

Quantitative real-time PCR (qPCR) was performed using an ABI Prism 7900 sequence detection system and a TaqMan universal PCR master mix kit (Life Technologies), as described previously. Each qPCR reaction contained 10 μL of reverse-transcriptase reaction mix, 25 μL of 2× TaqMan universal PCR master mix, 0.2 μmol/L probe, and 0.6 μmol/L primers. Primer and probe design for the qPCR was performed using Applied Biosystems Primer Express software version 2 (Life Technologies). The following primers were used: MLCK-specific primers, forward 5′-AGGAAGGCAGCATTGAGGTTT-3′ and reverse 5′-GCTTTCAGCAGGCAGAGGTAA-3′; MLCK-specific probe, FAM 5′-TGAAGATGCTGGCTCC-3′ TAMRA; internal control GAPDH-specific primers, forward 5′-CCACCCATGGCAAATTCC-3′ and reverse 5′-TGGGATTTCCATTGATGACCAG-3′; and GAPDH-specific probe, JOE 5′-TGGCACCGTCAAGGCTGAGAACG-3′ TAMRA. All runs were performed according to the default PCR protocol (50°C for 2 minutes and 95°C for 10 minutes, followed by 40 cycles of 95°C for 15 seconds, and then 60°C for 1 minute). For each sample, qPCR reactions were performed in triplicate, and the average $C_T$ was calculated. A standard curve was generated to convert the $C_T$ to copy numbers. Expression of MLCK mRNA was normalized with GAPDH mRNA expression. The average copy number of MLCK mRNA expression in control samples was set to 1.0. The relative expression of MLCK mRNA in treated samples was determined as a fold increase, relative to control samples.

### siRNA of ERK1/2 and Elk-1

Targeted siRNAs were purchased from Dharmacon (Thermo Scientific). Caco-2 monolayers were transiently transfected using DharmaFECT transfection reagent (Thermo Scientific). In brief, $5 \times 10^5$ cells/filter were seeded into a 12-well Transwell plate and grown to confluency. The Caco-2 monolayers were washed with PBS twice, and then 0.5 mL of Accell delivery medium (Thermo Scientific) was added to the apical compartment of each filter and 1.5 mL was added to the basolateral compartment of each filter. The siRNA of interest (5 ng) and DharmaFECT reagent (2 μL) were added to the apical compartment of each filter. The TNF-α experiments were performed at 96 hours after transfection. The efficiency of silencing was confirmed by Western blot analysis.

### ELISA-Based Determination of *in Vitro* ERK1/2 Kinase Activity

For ELISA, biotinylated myelin basic protein (MBP) was diluted in PBS and incubated on streptavidin-coated 96-well plates at 37°C for 1 hour. The plates were washed three times with PBS, incubated with blocking solution (1 mg/mL bovine serum albumin in PBS) at 37°C for 1 hour, and then washed three more times with PBS. Ninety microliters of kinase reaction buffer [20 mmol/L Tris/HCl (pH 7.5), 10 mmol/L $MgCl_2$, 50 mmol/L NaCl, 1 mmol/L dithiothreitol, 1 mmol/L NaF, 50 μmol/L ATP] provided by the manufacturer (MBL International, Woburn, MA) and 10 μL of samples containing immunoprecipitated ERK1/2 were added to each well, and the kinase reaction (phosphorylation of MBP) was performed at 37°C for 30 to 60 minutes. The reaction was stopped by removing the reaction mixtures and washing the plates three times with washing buffer [20 mmol/L Tris-HCl (pH 7.4), 0.5 mol/L NaCl, and 0.05% Tween 20]. The washed plates were incubated with 5 ng/mL anti−p-MBP antibody at room temperature for 1 hour. The plates were washed four times with washing buffer, and goat anti-rabbit IgG antibody (diluted 1:2000 in washing buffer) was added to the wells, and the plates were incubated at 37°C for 1 hour. The plates were washed four more times and incubated with 100 μL of substrate solution tetramethylbenzidine at 37°C for 5 to 15 minutes. To stop the reaction, 100 μL of stop solution containing 0.5 N $H_2SO_4$ was added. The absorbance at 450 nm was determined using a SpectraMax 190 microplate reader (Molecular Devices).

### Nuclear Extracts and ELISA for Transcription Factor Activation

Filter-grown Caco-2 monolayers were treated with 10 ng/mL TNF-α for 30 minutes. The Caco-2 monolayers were washed with ice-cold PBS, scraped, collected, and centrifuged at 20,817 × *g* for 30 seconds. The cell pellets were

resuspended in 200 μL of buffer A [10 mmol/L HEPES-KOH, 1.5 mmol/L $MgCl_2$, 10 mmol/L KCl, 0.5 mmol/L dithiothreitol, and 0.2 phenylmethylsulfonyl fluoride (pH 7.9)] and incubated on ice for 15 minutes. After centrifugation at 14,000 rpm for 30 seconds, pelleted nuclei were resuspended in 30 μL of buffer C [20 mmol/L HEPES-KOH (25% glycerol), 420 mmol/L NaCl, 1.5 mmol/L $MgCl_2$, 0.2 mmol/L EDTA, 0.5 mmol/L dithiothreitol, and 0.2 mmol/L phenylmethylsulfonyl fluoride (pH 7.9)]. After incubation on ice for 20 minutes, the lysates were centrifuged at 14,000 rpm for 20 minutes. Protein concentrations were determined using the Bradford method. The Elk-1 DNA-binding assay was performed using TransAM ELISA-based kits from Active Motif (Carlsbad, CA) according to the manufacturer's protocol. In brief, the binding reactions contained 1 pmol/L biotinylated probe (Integrated DNA Technologies, Coralville, IA) and 5 μg of nuclear extract in complete binding buffer with a total volume of 50 μL. After 30 minutes of incubation, the solution was transferred to an individual well on 96-well plate and incubated for 1 hour. The appropriate antibody (2 μg/mL) was added to the well to bind the target protein in nuclear extract. After incubation for 1 hour, the antibody was removed, and 100 μL of horseradish peroxidase—conjugated secondary antibody was added to the well and incubated for 1 hour. Subsequently, 100 μL of developing solution was added for 2 to 10 minutes, and then 100 μL of stop solution was added. The absorbance at 450 nm was determined using a SpectraMax 190 microplate reader (Molecular Devices).

## Cloning of the Full-Length *MLCK* Promoter Region and Deletion Constructs

The *MLCK* promoter region was cloned using a GenomeWalker system (Clontech Laboratories, Mountain View, CA). A 2091-bp DNA fragment (−2109 to −18) was amplified by PCR. The amplification condition was 94°C for 2 minutes, followed by 43 cycles at 94°C for 1 minute, 50°C for 1 minute, and 72°C for 2 minutes, and then 72°C for 5 minutes. The resultant PCR product was digested with HindIII and KpnI and inserted into pGL3-basic luciferase reporter vector (Promega, Madison, WI). The sequence was confirmed at the University of New Mexico DNA Research Services. Construction of *MLCK* promoter reporter plasmids was performed using the pGL3-basic luciferase reporter vector. Deletions of *MLCK* promoter were performed according to the PCR method. The PCR conditions were 94°C for 2 minutes, followed by 43 cycles at 94°C for 1 minute, 50°C for 1 minute, and 72°C for 2 minutes, and then 72°C for 5 minutes. The resultant PCR products were cloned into pGL3-basic luciferase reporter vector and the sequences were confirmed.

## Transfection of DNA Constructs and Assessment of Promoter Activity

DNA constructs of *MLCK* promoters were transiently transfected into Caco-2 cells using Lipofectamine 2000 transfection reagent (Life Technologies). *Renilla* luciferase vector (pRL-TK; Promega) was cotransfected with each plasmid construct, as an internal control. Cells ($5 \times 10^5$ per filter) were seeded into a six-well Transwell plate and grown to confluency. The Caco-2 monolayers were washed with PBS twice, and then 1.0 mL of Opti-MEM medium was added to the apical compartment of each filter and 1.5 mL was added to the basolateral compartment of each filter. One microgram of each plasmid construct and 0.25 μg of pRL-TK or 2 μL of Lipofectamine 2000 (Life Technologies) were preincubated in 250 μL of Opti-MEM medium. After 5 minutes of incubation, the two solutions were mixed and incubated for another 20 minutes, and the mixture was added to the apical compartment of each filter. After incubation for 3 hours at 37°C, 500 μL of Dulbecco's modified Eagle's medium containing 10% fetal bovine serum were added to both sides of the filter to reach a 2.5% final concentration of fetal bovine serum. Subsequently, the medium was replaced with normal Caco-2 growth medium at 16 hours after transfection.

Specific experiments were performed at 48 hours after transfection. At the completion of specific experimental treatments, Caco-2 cells were washed twice with 1 mL of ice-cold PBS, and 400 μL of 1× passive lysis buffer was added; cells were then incubated at room temperature for 15 minutes, scraped, transferred into an Eppendorf tube, and centrifuged for 15 seconds at 13,000 rpm in a microcentrifuge. Luciferase activity was determined using a dual luciferase assay kit (Promega). Twenty microliters of the supernatant was used for each assay. Luciferase values were determined using a Lumat LB 9507 luminometer (Berthold Technologies, Oak Ridge, TN; Bad Wildbad, Germany). The value of reporter luciferase activities were then divided by that of *Renilla* luciferase activities to normalize for differences in transfection efficiencies. The average activity value of the control samples was set to 1.0. The luciferase activity of *MLCK* promoter in treated samples was determined relative to control samples.

## Site-Directed Mutagenesis

Mutagenesis of *MLCK* promoter was performed using an Invitrogen GeneTailor site-directed mutagenesis system (Life Technologies). In brief, primers were generated that included the mutation site flanked by a wild-type sequence on either side (mutant primer, forward 5′-CTGCAGGAAGGCAGCTCCCACAATTCCTTCTTTCTACCCCTGCCA-3′ and reverse 5′-TGGGAGCTGCCTTCCTGCAGGTGAAAGGCA-3′). A PCR reaction produced a new complete copy of the plasmid containing the mutation coded for by the primers. The linear PCR product was subsequently transformed into DH5-T1 *Escherichia coli*, which circularized the PCR product and digested any remaining parent plasmid. DNA sequence was then verified at the University of New Mexico DNA Research Services.

### *In Vivo* Mouse Intestinal Permeability Measurements

The Laboratory Animal Care and Use Committee at the University of New Mexico approved all experimental protocols.

Mouse intestinal permeability was measured by recycling small intestinal perfusion, as described previously.[29–31] After the experimental period, mice were anesthetized with isoflurane. After midline incision of the abdomen, 5 cm of intestine segment was isolated and cannulated at the proximal and distal ends with polyethylene tubing (0.76 mm internal diameter). Flushing solution [140 mmol/L NaCl, 10 mmol/L HEPES (pH 7.4)] warmed to 37°C was first perfused through the intestine at 1 mL/minute for 20 minutes, followed by air flush to remove residual contents using an external pump (Bio-Rad Laboratories). This was followed by perfusion of 5 mL of perfusate solution [85 mmol/L NaCl, 10 mmol/L HEPES, 20 mmol/L sodium ferrocyanide, 5 mmol/L KCl, 5 mmol/L $CaCl_2$ (pH 7.4)] containing Texas Red–labeled dextran 10K (10 kDa) in a recirculating manner at 0.75 mL/minute for 2 hours. The abdominal cavity was covered with moistened gauze, and body temperature was measured via rectal thermometer; body temperature was maintained at 37.5 ± 0.5°C using a heating lamp. Aliquots (1 mL) of test solution were removed at the beginning and end of the perfusion. After perfusion, the animal was sacrificed, the perfused intestine segment was excised, and the length was measured. The excised intestinal loop was then snap-frozen in optimal cutting temperature compound or was used for protein and RNA analysis. Ferrocyanide concentration in the perfusate was measured using a colorimetric assay. Texas Red–labeled dextran 10K concentration was measured using an excitation wavelength of 595 nm and an emission wavelength of 615 nm in a microplate reader.

Probe clearance was calculated as $C_{probe} = (C_i V_i - C_f V_f)/C_{avg} TL$, where $C$ is the probe concentration and $V$ is the perfusate volume; the subscripts i, f, and avg indicate initial measured, final, and average values; $T$ is perfusion time in hours; and $L$ is the length of the perfused intestine section in centimeters. $V_f$ was calculated as $V_i([\text{ferrocyanide}]_i/[\text{ferrocyanide}]_f)$. $C_{avg}$ was calculated as $(C_i - C_f)/\ln(C_i/C_f)$.

### Animal Surgery and *in Vivo* Transfection of ERK1/2 and Elk-1 siRNA

Mice were fasted for 24 hours before the surgery. Mice were anesthetized with isoflurane (4% for surgical induction and 1% for maintenance) using oxygen as carrier during surgical procedures. Surgical procedures were performed using sterile technique. The abdomen was opened by a midline incision, and a 6-cm segment of intestine was isolated at the proximal and distal ends and tied with sutures. Next, 0.5 mL of siRNA transfection solution (containing Accell medium, 2.5 nmol ERK1/2 or Elk-1 siRNA, and 50 μL of Lipofectamine 2000 transfection reagent) was introduced into the lumen of the isolated intestinal segment using a 30-G needle for a 1-hour transfection period. Control animals underwent sham surgery, for which the siRNA transfection solution contained Accell medium, 2.5 nmol nontarget siRNA, and 50 μL of Lipofectamine 2000 transfection reagent. The abdominal cavity was covered with moistened gauze. Body temperature was monitored continuously with a rectal probe and was maintained at 37.5 ± 0.5°C using a heating pad. After the 1-hour transfection period, each end of the intestinal segment was untied, the intestine was placed back into the abdominal cavity, and the abdomen was closed. At 3 days after transfection, functional studies of intestinal epithelial barrier were performed. The surgery and the *in vivo* transfection procedures had no effect on food intake or body weight of the animals during the experimental period. Animal weight averaged between 23 and 25 g during the experimental period.

### Statistical Analysis

Statistical significance of differences between mean values was assessed with Student's *t*-tests for unpaired data and analysis of variance analysis whenever required. All reported significance levels represent two-tailed $P$ values. A $P$ value of $<0.05$ was used to indicate statistical significance. Each experiment was performed in triplicate or quadruplicate ($n = 3$ or 4), and all experiments were repeated at least three times to ensure reproducibility.

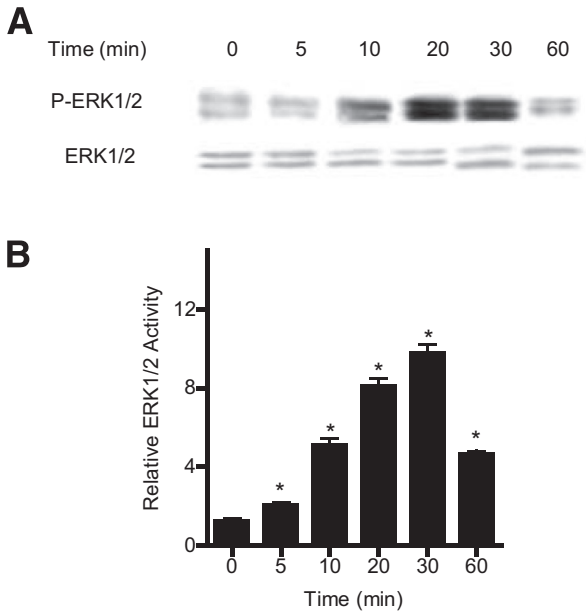


**Figure 1** Effect of TNF-α on filter-grown Caco-2 ERK1/2 activation. **A:** TNF-α (10 ng/mL) causes a time-dependent increase in Caco-2 ERK1/2 phosphorylation; total ERK1/2 was used for equal protein loading. **B:** TNF-α causes a time-dependent increase in ERK1/2 activity as determined by ELISA-based *in vitro* kinase activity using MBP as the substrate. Data are expressed as means ± SEM. $n = 4$. *$P < 0.001$ versus control.

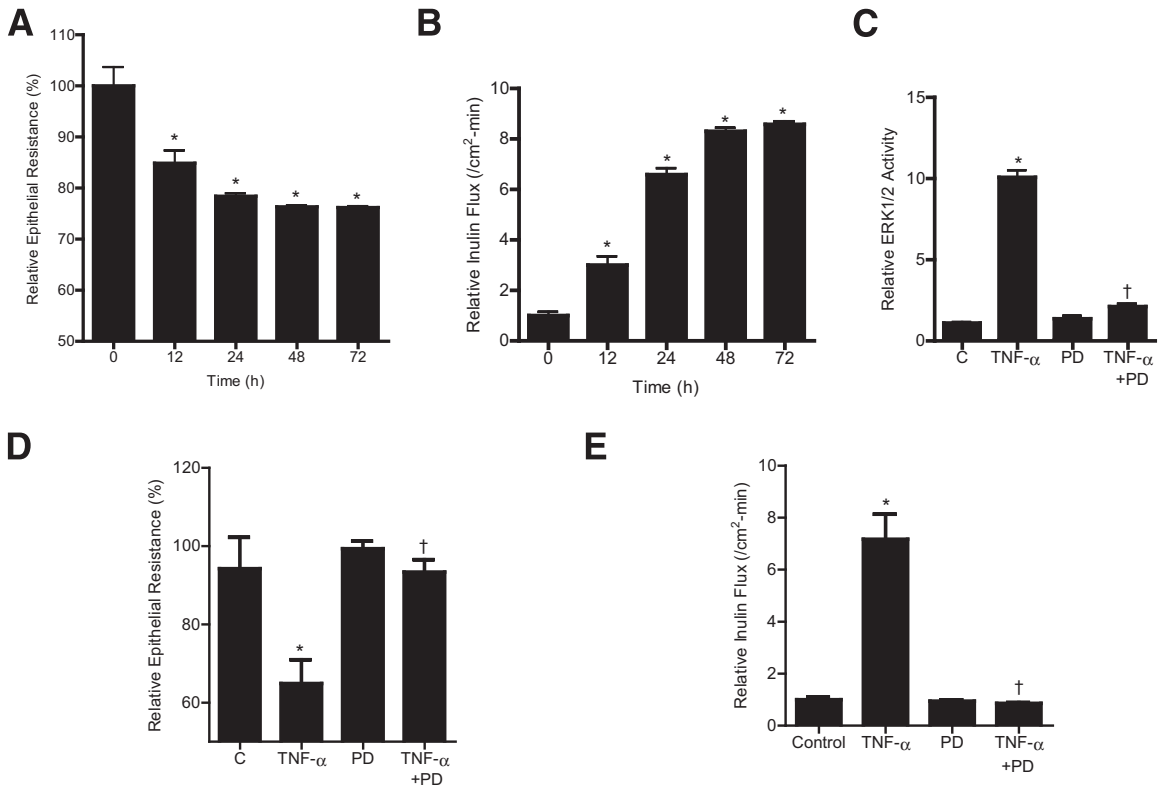


**Figure 2** Effect of ERK1/2 inhibition by the pharmacological inhibitor PD 98059 (100 μmol/L) on Caco-2 ERK1/2 activity, TER, and paracellular permeability. **A** and **B:** TNF-α (10 ng/mL) causes a time-dependent decrease in Caco-2 TER (**A**) and a time-dependent increase in mucosal-to-serosal flux of the paracellular marker inulin (**B**). **C:** Pretreatment with 100 μmol/L PD 98059 for 1 hour before TNF-α treatment inhibits the TNF-α—induced increase in ERK1/2 *in vitro* kinase activity. **D:** PD 98059 prevents the TNF-α—induced decrease in Caco-2 TER. **E:** Pretreatment with PD 98059 prevents the TNF-α—induced increase in mucosal-to-serosal inulin flux. Data are expressed as means ± SEM. $n = 4$ (**C**); $n = 6$ (**A**, **B**, **D**, and **E**). *$P < 0.001$ versus control. †$P < 0.001$ versus TNF-α treatment.

## Results

### The TNF-α—Induced Increase in Caco-2 TJ Permeability Is Regulated by MAP Kinase Activation

We examined the possibility that the TNF-α—induced increase in Caco-2 TJ permeability is mediated by MAP kinase activation. Because TNF-α has been shown to activate MAP kinases ERK1/2 and p38 kinase in various cell types,[24,25] these two kinase pathways were targeted. The time-course effect of 10 ng/mL TNF-α on ERK1/2 or p38 kinase activation was determined by measuring ERK1/2 phosphorylation in filter-grown Caco-2 monolayers. TNF-α caused a rapid increase in ERK1/2 phosphorylation in Caco-2 cells, starting at about 10 minutes and continuing up to 60 minutes, as determined by p-ERK1/2 immunoblotting (Figure 1A). In contrast, TNF-α did not have a significant effect on p38 kinase phosphorylation (Supplemental Figure S1). The total ERK1/2 level was not affected by the TNF-α treatment (Figure 1A). The effect of TNF-α on ERK1/2 kinase activity was also confirmed by an ELISA-based *in vitro* kinase assay. The kinase activity of immunoprecipitated ERK1/2 was directly measured *in vitro* using MBP as the substrate. TNF-α caused a rapid increase in Caco-2 ERK1/2 kinase activity, starting at about 5 to 10 minutes (Figure 1B). These data suggested that TNF-α causes a rapid activation (within minutes) of ERK1/2 (but not p38 kinase) in Caco-2 monolayers.

To determine the requirement of ERK1/2 activation in the TNF-α—induced increase in Caco-2 TJ permeability, the effect of ERK1/2 inhibition was examined. Caco-2 TJ permeability was determined by measuring Caco-2 TER or transepithelial flux of the paracellular marker inulin.[26,28] TNF-α caused a time-dependent decrease in Caco-2 TER and an increase in transepithelial flux of inulin (Figure 2, A and B). At 100 μmol/L, the ERK1/2 inhibitor PD 98059 inhibited TNF-α—induced activation of ERK1/2, as assessed by *in vitro* kinase activity (Figure 2C), and prevented the decrease in TER (Figure 2D) and increase in inulin flux (Figure 2E). In contrast, the p38 kinase inhibitor SB 203580 did not have any effect on the TNF-α—induced increase in Caco-2 TJ permeability (Supplemental Figure S2). These results suggested that ERK1/2 activation is required for the TNF-α—induced increase in Caco-2 TJ permeability.

To further confirm the requirement of ERK1/2 for the effect of TNF-α on Caco-2 TJ permeability, ERK1/2 expression was selectively knocked down by siRNA transfection. Transfection of ERK1/2 siRNA caused a near-complete depletion of ERK1/2 in filter-grown Caco-2

monolayers (Figure 3A). The siRNA-induced knockdown of ERK1/2 prevented the TNF-α–induced decrease in Caco-2 TER (Figure 3B) and increase in inulin flux (Figure 3C), confirming the requirement of ERK1/2 in the TNF-α–induced increase in Caco-2 TJ permeability.

## ERK1/2 Signaling Pathway Is Involved in the Regulation of *MLCK* Gene and Protein Expression

Previous studies from our research group and others have shown that the TNF-α–induced increase in Caco-2 TJ permeability is mediated by an increase in MLCK protein expression and activity.[6,17–19] However, the intracellular signaling pathways or the molecular mechanisms involved in the TNF-α regulation of *MLCK* gene and protein expression remain unclear. In the present study, we examined the involvement of the ERK1/2 signaling pathway in TNF-α up-regulation of *MLCK* gene and protein expression. TNF-α caused an increase in Caco-2 MLCK mRNA and protein expression (Figure 4, A and B). The inhibition of ERK1/2 with the pharmacological inhibitor PD 98059 (100 μmol/L) prevented the TNF-α–induced increase in MLCK mRNA and protein expression (Figure 4, C and D). Similarly, siRNA-induced knockdown of Caco-2 ERK1/2 also inhibited the TNF-α–induced increase in MLCK mRNA and protein level (Figure 4, E and F). Taken together, these data suggested that the ERK1/2 signaling pathway mediates the TNF-α modulation of MLCK mRNA and protein expression.

## Transcription Factor Elk-1 Regulates *MLCK* Gene Activity and TJ Permeability

Next, we examined the nuclear transcription factor and the molecular determinants that regulate the TNF-α–induced increase in *MLCK* gene activity and Caco-2 TJ permeability. Nuclear transcription factor Elk-1, a direct substrate of ERK1/2, binds to serum response element on a promoter region and regulates gene transcription.[32–34] Using PromoterInspector software (Genomatix, Munich, Germany), we identified two Elk-1 binding motifs or serum response elements on the *MLCK* promoter region. The effect of TNF-α on Elk-1 activation was examined by measuring Elk-1 phosphorylation and by ELISA-based DNA binding assay. TNF-α caused a time-dependent increase in Caco-2 Elk-1 phosphorylation (Ser383) (Figure 5A). TNF-α also caused an increase in binding of activated Elk-1 (in the nuclear fraction) to the Elk-1 binding sequence on the DNA probe (Figure 5B). The ERK1/2 inhibitor PD 98059 inhibited the TNF-α–induced increase in Elk-1 phosphorylation and the DNA binding of Elk-1 (Figure 5, C and D).

We then examined the regulatory role of Elk-1 on *MLCK* promoter activity, using siRNA silencing of Elk-1 in Caco-2 monolayers. The transfection of filter-grown Caco-2 monolayers with Elk-1 siRNA caused a near-complete depletion of Elk-1 expression (Figure 6A). TNF-α caused an increase in *MLCK* promoter activity, and siRNA knockdown of

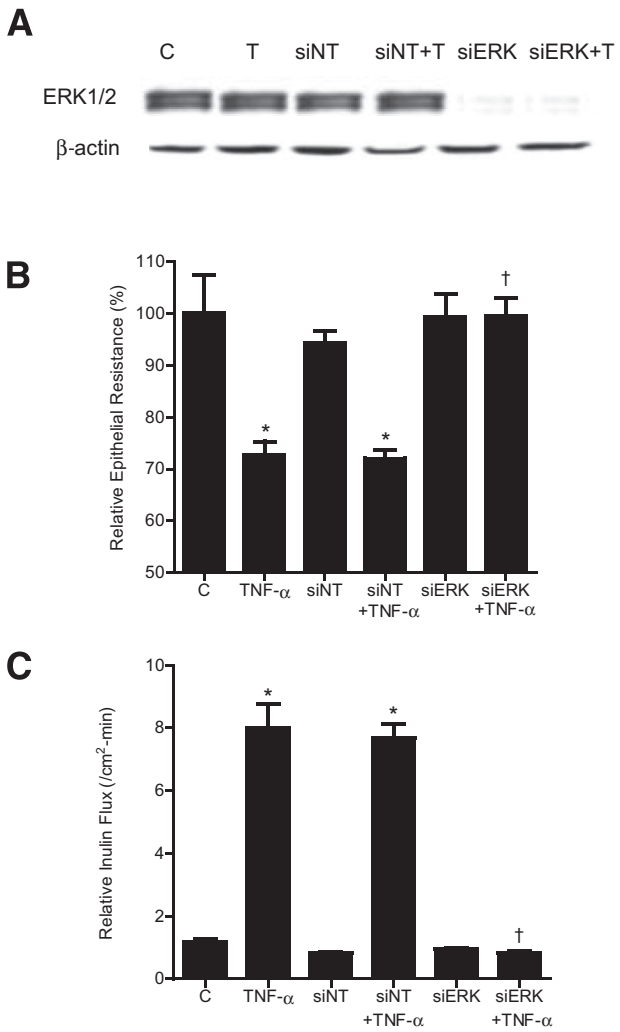


**Figure 3** Effect of siRNA-induced ERK1/2 knockdown on the TNF-α–induced increase in Caco-2 TJ permeability. **A**: ERK1/2 siRNA transfection results in a near-complete depletion in ERK1/2 protein expression. **B** and **C**: ERK1/2 siRNA transfection prevents the TNF-α–induced decrease in Caco-2 TER (**B**) and the TNF-α–induced increase in inulin flux (**C**). Data are expressed as means ± SEM. $n = 6$. $^{*}P < 0.001$ versus control. $^{\dagger}P < 0.001$ versus TNF-α treatment.

Elk-1 prevented the increase in *MLCK* promoter activity (Figure 6B). siRNA knockdown of Elk-1 also inhibited the TNF-α–induced increase in MLCK at the mRNA and protein levels (Figure 6, C and D) and the increase in Caco-2 TJ permeability (Figure 6, E and F). Taken together, these data suggested that Elk-1 activation is required for the increase in *MLCK* gene activity and the subsequent increase in Caco-2 TJ permeability.

## Elk-1 Regulation of *MLCK* Promoter

Next, we determined the molecular determinants that mediate the TNF-α modulation of *MLCK* promoter activity. As noted above, two serum response elements or Elk-1 binding sequences were identified on the *MLCK* promoter region: site A, between −1118 and −1102 (5′-TGGCCTTCCTCCCTC-3′),

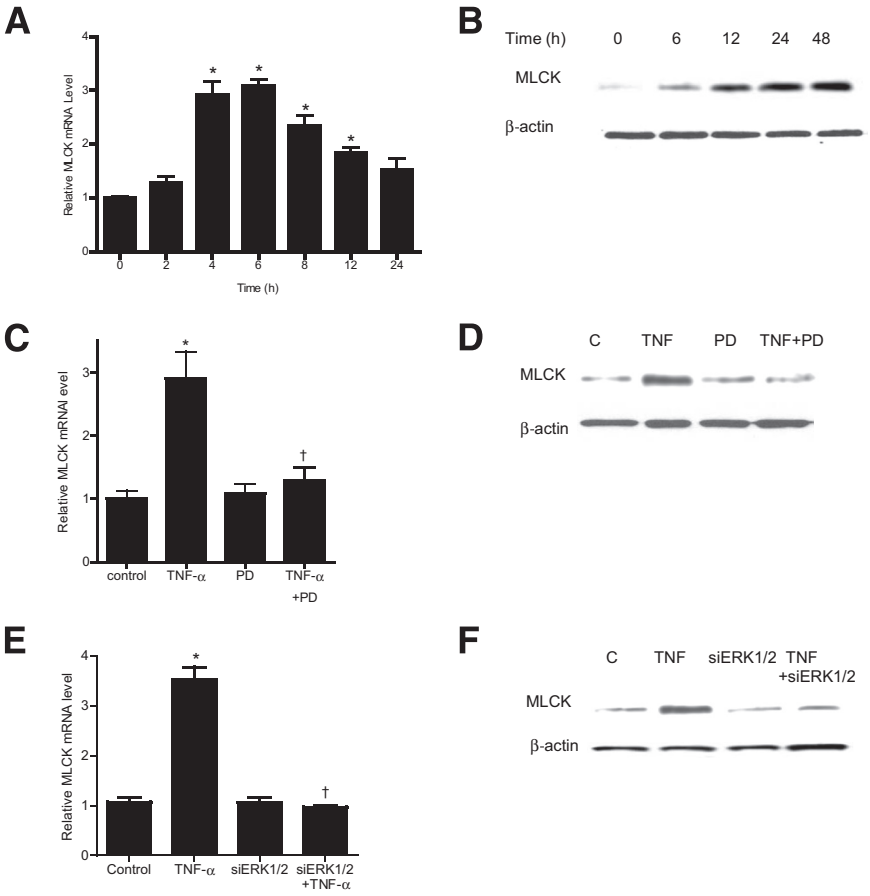


**Figure 4** Effect of ERK1/2 inhibition on the TNF-α—induced increase in Caco-2 *MLCK* gene and protein expression. **A:** TNF-α causes a time-dependent increase in MLCK mRNA levels. The average copy number of MLCK mRNA in controls was $4.63 \times 10^{11}$. **B:** TNF-α causes a time-dependent increase in MLCK protein expression. **C:** Pretreatment with the ERK1/2 inhibitor PD 98059 1 hour before TNF-α treatment prevents the TNF-α—induced increase in MLCK mRNA levels. **D:** The ERK1/2 inhibitor PD 98059 prevents the TNF-α—induced up-regulation of MLCK protein expression. **E:** siRNA-induced knockdown of ERK1/2 prevents the TNF-α—induced increase in MLCK mRNA. **F:** ERK1/2 siRNA transfection prevents the TNF-α—induced increase in MLCK protein expression. Data are expressed as means ± SEM. $n = 8$. Experimental period, 6 hours (**C** and **E**). $^{*}P <$ 0.001 versus control. $^{\dagger}P < 0.001$ versus TNF-α treatment.

and site B, between −310 and −296 (5′-GAAAATGGAA-GTCCAAG-3′) (Figure 7A). Three *MLCK* promoter deletion constructs were generated that contained both Elk-1 binding motifs α and β (full-length promoter region) and DNA constructs that contained only the downstream binding site B. Two deletion constructs encoding the site B were generated: MLCK −926, which encodes the promoter region upstream of the binding sequence B (−310 to −296) and MLCK −313, which encodes the sequence B but does not encode the upstream promoter region beyond −313.

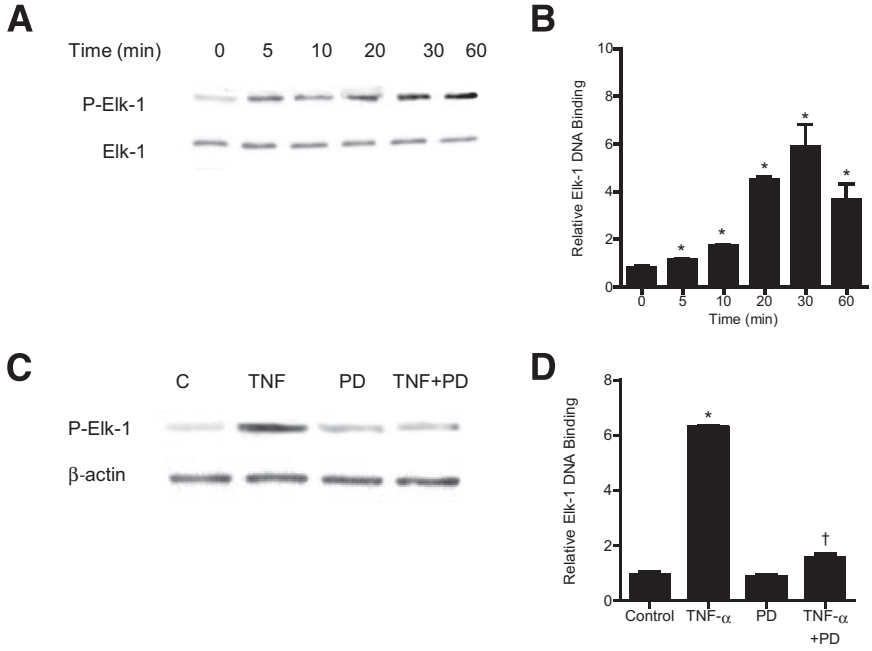


**Figure 5** Effect of TNF-α on Elk-1 activation. **A:** TNF-α treatment results in a time-dependent increase in Elk-1 phosphorylation. **B:** TNF-α causes a time-dependent increase in Elk-1 activity as determined by ELISA-based binding assay. **C:** Pretreatment with the ERK1/2 inhibitor PD 98059 for 1 hour before TNF-α treatment prevents TNF-α—induced Elk-1 phosphorylation. **D:** Pretreatment with PD 98059 for 1 hour before TNF-α treatment prevents TNF-α—induced binding of Elk-1 to its binding site on DNA probe as determined by DNA ELISA binding assay. Data are expressed as means ± SEM. $n = 4$. $^{*}P < 0.001$ versus control. $^{\dagger}P < 0.001$ versus TNF-α treatment.

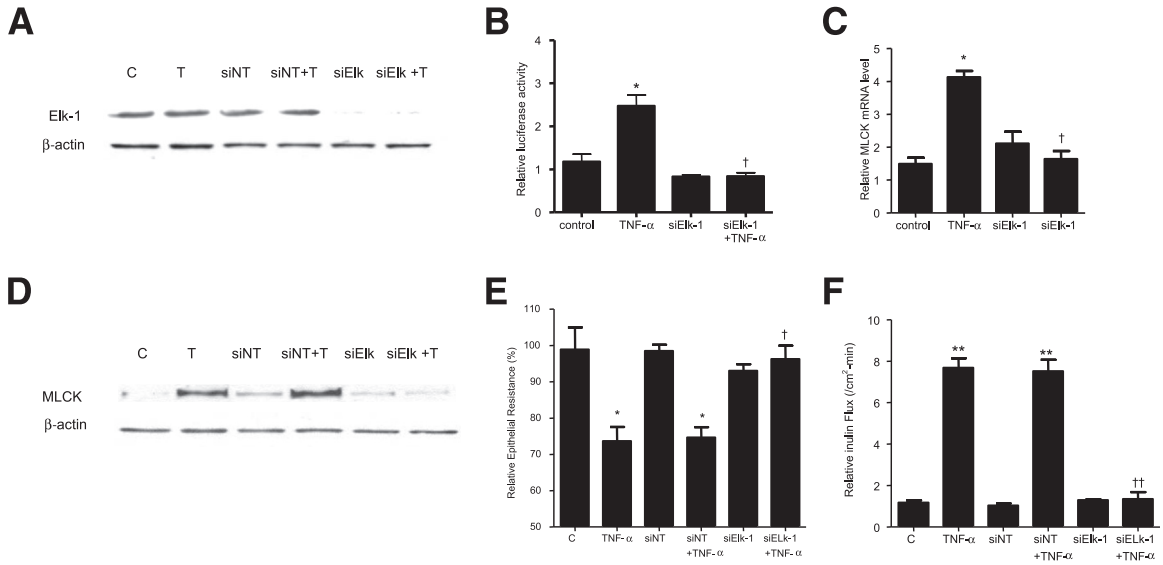


**Figure 6** **A:** Elk-1 siRNA transfection results in a near-complete depletion in Elk-1 protein expression in filter-grown Caco-2 monolayers. **B:** Elk-1 siRNA transfection significantly prevents the TNF-α–induced increase in Caco-2 *MLCK* promoter activity. **C:** Elk-1 silencing by siRNA prevents the TNF-α–induced increase in Caco-2 MLCK mRNA levels. **D:** Elk-1 silencing by siRNA transfection abolishes TNF-α up-regulation of Caco-2 MLCK protein expression. **E:** Elk-1 siRNA transfection prevents the TNF-α–induced decrease in Caco-2 TER. **F:** Elk-1 silencing inhibits the TNF-α–induced increase in mucosal-to-serosal inulin flux. Data are expressed as means ± SEM. $n = 4$ (**E**); $n = 5$ (**B** and **F**); $n = 8$ (**C**). $^{*}P < 0.001$, $^{**}P < 0.0001$ versus control. $^{\dagger}P < 0.001$, $^{\dagger\dagger}P < 0.0001$ versus TNF-α treatment.

TNF-α treatment produced a similar proportional increase in all three DNA constructs (Figure 7, B and C), suggesting that the presence of the binding site B alone was sufficient to cause an increase in *MLCK* promoter activity and that site A is not required. To validate the requirement of site B in the regulation of *MLCK* promoter activity, binding site B was mutated via site-directed mutagenesis. The mutation of site B inhibited the TNF-α–induced increase in promoter activity (Figure 8A), confirming that site B was necessary for the up-regulation of promoter activity. Lastly, the effect of siRNA-induced silencing of Elk-1 on the TNF-α–induced increase in *MLCK* promoter activity in MLCK −313 was determined. The siRNA-induced knockdown of Elk-1 inhibited the TNF-α–induced increase in promoter activity in MLCK −313 (Figure 8B). Taken together, these data indicated that Elk-1 binding site B located within the minimal promoter region is the regulatory site responsible for TNF-α–induced activation of *MLCK* promoter activity.

## The Role of ERK1/2 and Elk-1 in the TNF-α–Induced Increase in Mouse Intestinal Permeability *in Vivo*

To this point, our studies suggested that ERK1/2 signaling cascade activation is required for the TNF-α modulation of *MLCK* and TJ permeability in filter-grown Caco-2 monolayers; however, the *in vivo* relevance of these findings remained unclear. We therefore examined the involvement of the ERK1/2 signaling pathway in TNF-α modulation of mouse intestinal permeability by recycling intestinal perfusion of mouse small intestine *in vivo*.[31] Intraperitoneal injection of 5 μg of TNF-α caused an increase in intestinal permeability, as assessed by mucosal-to-serosal flux of a commonly used paracellular marker, Texas Red–dextran 10K (Figure 9A). TNF-α treatment resulted in a time-dependent increase in ERK1/2 phosphorylation and activation in the small intestinal tissue (Figure 9, B and C). TNF-α also caused an increase in intestinal MLCK mRNA and protein expression (Figure 9, D and E). To confirm the regulatory role of the ERK1/2 pathway in intestinal MLCK expression and intestinal permeability *in vivo*, intestinal ERK1/2 expression was silenced by *in vivo* siRNA transfection of small intestine, using a recently described *in vivo* transfection methodology.[29,31] In brief, 6 cm of mouse jejunum was isolated using sutures, and the mucosal surface was exposed to transfection solution containing ERK1/2 siRNA for 1 hour; the sutures were then removed, the intestinal segment was reinserted into the original location in the abdomen, and the abdominal cavity was closed with sutures. After 2 days, to allow for ERK1/2 depletion, mice were treated with TNF-α; intestinal permeability studies were performed on day 3. *In vivo* ERK1/2 siRNA transfection resulted in a near-complete knockdown of ERK1/2 in the intestinal tissue (Figure 10A). The *in vivo* siRNA knockdown of ERK1/2 prevented the TNF-α–induced increase in intestinal MLCK expression (Figure 10B) and increase in intestinal permeability (Figure 10C). Taken together, these results suggest a regulatory role for the ERK1/2 kinase pathway in TNF-α modulation of intestinal MLCK expression and intestinal permeability *in vivo*.

Next, we examined the possible involvement of Elk-1 in TNF-α modulation of mouse intestinal permeability *in vivo*. TNF-α administration caused a time-dependent increase in

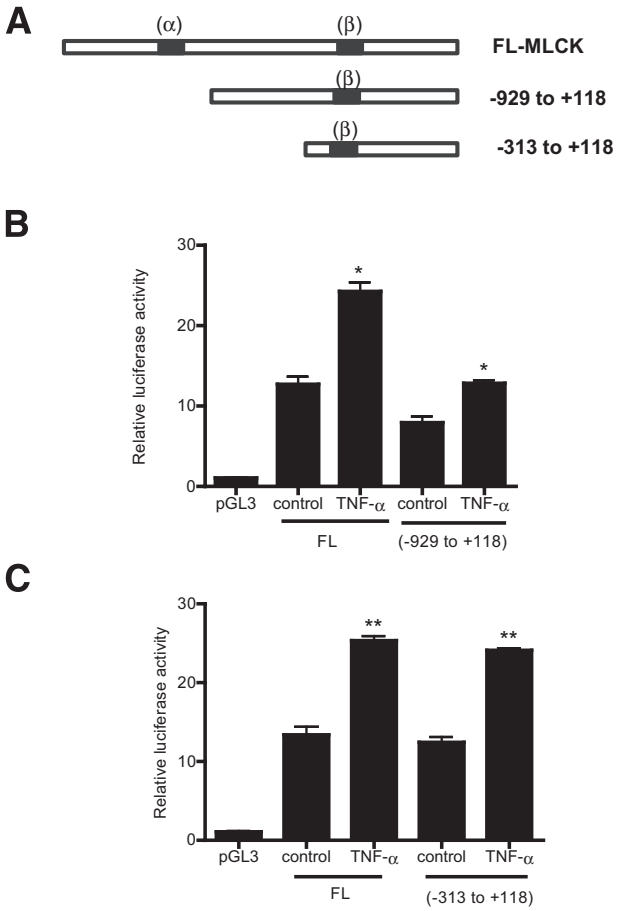


**Figure 7** **A:** Schematic diagram of the DNA constructs of *MLCK* promoter (−2109 to −18) containing different combinations of Elk-1 binding sites. The Elk-1 binding sites α (GAAAATGGAAGTCCAAG) and β (TGGCCTTCCTCCCTC) are indicated (**black bands**). **B:** TNF-α causes an increase in MLCK luciferase activity on the deletion construct of *MLCK* promoter region (−929 to +118) lacking the downstream Elk-1 binding site α, compared with the full-length (FL) construct. **C:** TNF-α treatment causes a significant increase in *MLCK* promoter activity of the deletion construct (−313 to +118) containing only the cis-binding site β in Caco-2 monolayers. Data are expressed as means ± SEM. $n = 8$. $^{*}P < 0.001$, $^{**}P < 0.0001$ versus control.

intestinal tissue Elk-1 phosphorylation (Figure 11A). Time-course studies indicated that TNF-α–induced ERK1/2 activation (Figure 9, B and C) preceded Elk-1 activation. We also examined the effect of siRNA-induced silencing of Elk-1 on mouse small intestinal MLCK expression and mouse intestinal permeability. siRNA-induced knockdown of Elk-1 *in vivo* (Figure 11B) resulted in inhibition of the TNF-α–induced increase in intestinal tissue MLCK protein expression and mouse intestinal permeability (Figure 11, B and C). siRNA-induced knockdown of ERK1/2 also inhibited the increase in Elk-1 phosphorylation, confirming that ERK1/2 activation is required for the intestinal tissue Elk-1 activation *in vivo* (Figure 11D). Taken together, these data suggested that the TNF-α–induced increase in mouse intestinal permeability *in vivo* is also mediated by ERK1/2 activation of Elk-1 and by Elk-1–dependent increase in MLCK expression.

## Discussion

The intracellular signaling pathways that mediate TNF-α modulation of intestinal epithelial TJ barrier remain unclear. Previous studies from our research group and others indicated that the TNF-α modulation of intestinal TJ barrier is dependent on *MLCK* gene activation and protein expression.[6,17–19] With the present studies, we have extended our previous findings to delineate the intracellular signaling cascades that regulate the TNF-α modulation of intestinal permeability *in vitro* and *in vivo*.

The MAP kinase p38 and ERK1/2 pathways play an important role in mediating many of the TNF-α–induced immune responses,[24,25] and the ERK1/2 and p38 kinase pathways are involved in the regulation of growth, differentiation, apoptosis, and inflammatory responses.[25,35] However, the involvement of MAP kinase pathways in TNF-α modulation of intestinal TJ permeability *in vitro* and *in vivo* had not been reported previously. We therefore investigated the possibility that MAP kinase pathways may play a regulatory role in the effect of TNF-α on intestinal TJ permeability. Our results indicate that TNF-α causes activation of ERK1/2, but not p38 kinase, and that targeted inhibition of ERK1/2 kinase activity (but not p38 kinase) prevents the TNF-α–induced increase in Caco-2 TJ permeability, suggesting that the ERK1/2 signaling pathway (but not the

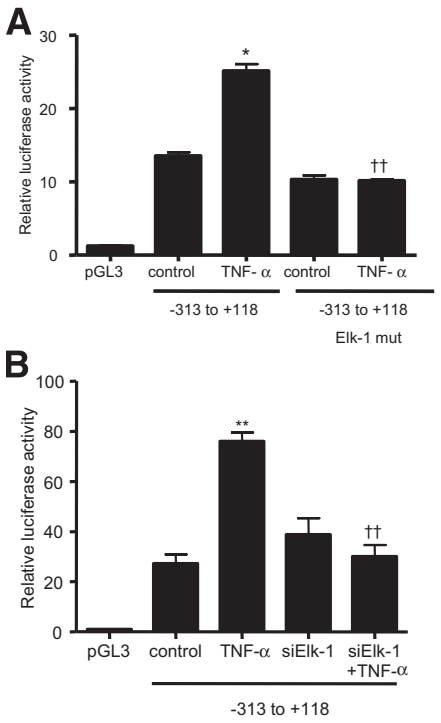


**Figure 8** **A:** Site-directed mutagenesis of the Elk-1 binding site β (5′-CAATTCCTTCTTTCT-3′) on MLCK −313 prevents the TNF-α–induced increase in MLCK −313 promoter activity. **B:** Elk-1 silencing completely prevents the TNF-α–induced increase in MLCK 313 promoter activity. Data are expressed as means ± SEM. $n = 6$. $^{*}P < 0.001$, $^{**}P < 0.0001$ versus control. $^{\dagger\dagger}P < 0.0001$ versus TNF-α treatment.

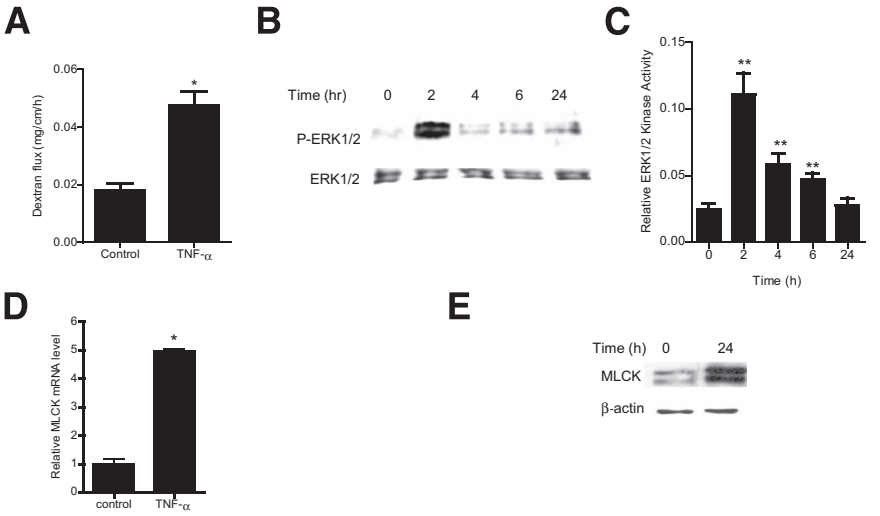


**Figure 9** Effect of TNF-α on the ERK1/2 signaling pathway in mouse small intestinal tissue *in vivo*. **A:** TNF-α (5 μg) causes an increase in mouse intestinal mucosal-to-serosal flux of dextran 10K. **B:** TNF-α causes a time-dependent increase in ERK1/2 phosphorylation; total ERK1/2 was used for equal protein loading. **C:** TNF-α causes a time-dependent increase in mouse intestinal ERK1/2 activity as determined by ELISA-based assay. **D:** TNF-α causes an increase in mouse MLCK mRNA levels. **E:** TNF-α causes an increase in mouse MLCK protein expression. Data are expressed as means ± SEM. $n = 6$ (**C** and **D**); $n = 8$ (**A**). Experimental period, 24 hours (**A**, **D**, and **E**). $^{*}P < 0.001$, $^{**}P < 0.0001$ versus control.

p38 kinase pathway) mediates the increase in Caco-2 TJ permeability.

These findings contradict recent data from our research group showing that IL-1β modulation of intestinal epithelial TJ barrier is dependent on both ERK1/2 and p38 kinase activation.[36,37] Those studies indicated that IL-1β activation of the p38 kinase pathway is necessary for the IL-1β–induced increase in Caco-2 TJ permeability, and inhibition of p38 kinase activity prevented the IL-1β–induced increase in Caco-2 TJ permeability.[36] In contrast to earlier results with IL-1β, in the present studies TNF-α did not cause an activation of p38 kinase in Caco-2 monolayers, and the p38 kinase inhibitor SB 203580 did not affect the TNF-α–induced increase in Caco-2 TJ permeability. These results suggest that the effects of IL-1β and TNF-α on Caco-2 TJ barrier are regulated by distinct intracellular processes. Interestingly, the ERK1/2 signaling pathway has been shown to have different effects on intestinal epithelial TJ barrier. In studies using epidermal growth factor, ERK1/2 activation mediated the intestinal TJ barrier enhancement.[38] Similarly, probiotic enhancement of intestinal TJ barrier also required ERK1/2 activation.[39] In mice, bile-induced enhancement of intestinal barrier also involved ERK1/2 activation.[40] On the other hand, mycotoxin-induced and IL-1β–induced increases in intestinal epithelial TJ permeability require ERK1/2 activation.[37,41] Thus, published data suggest that the ERK1/2 signaling pathway regulates both enhancement and attenuation of intestinal TJ barrier. How the ERK1/2 signaling pathway differentially regulates the intestinal TJ barrier requires further investigation.

Previous studies have shown that the TNF-α–induced increase in Caco-2 TJ permeability is associated with an increase in *MLCK* gene and protein expression, and inhibition of MLCK expression or MLCK activity prevented the increase in Caco-2 TJ permeability.[6,17–19] In the present studies, we examined the regulatory role of the ERK1/2 signaling cascade in mediating TNF-α modulation of *MLCK* gene activity and protein expression. ERK1/2 inhibitor or gene silencing studies demonstrated the requirement of ERK1/2 activation in the TNF-α–induced increase in *MLCK* gene activity and protein expression. As has been shown previously,[6,19] the increase in MLCK expression and

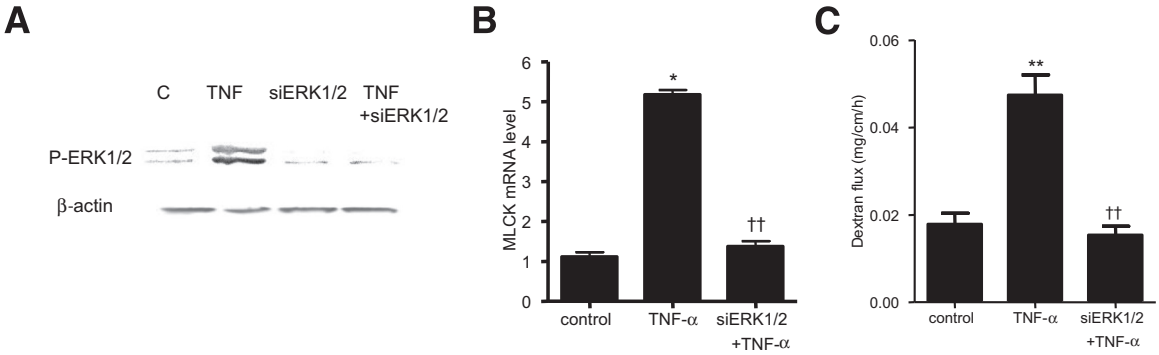


**Figure 10** **A:** ERK1/2 siRNA transfection prevents TNF-α–induced phosphorylation of ERK1/2. **B:** ERK1/2 siRNA transfection inhibits the TNF-α–induced increase in mouse MLCK mRNA levels. **C:** ERK1/2 silencing inhibits the TNF-α–induced increase in mucosal-to-serosal flux of dextran 10K. Data are expressed as means ± SEM. $n = 4$ (**B**); $n = 6$ (**C**). Experimental period, 2 hours (**A**); 24 hours (**B** and **C**). $^{*}P < 0.001$, $^{**}P < 0.0001$ versus control. $^{\dagger\dagger}P < 0.0001$ versus TNF-α treatment.

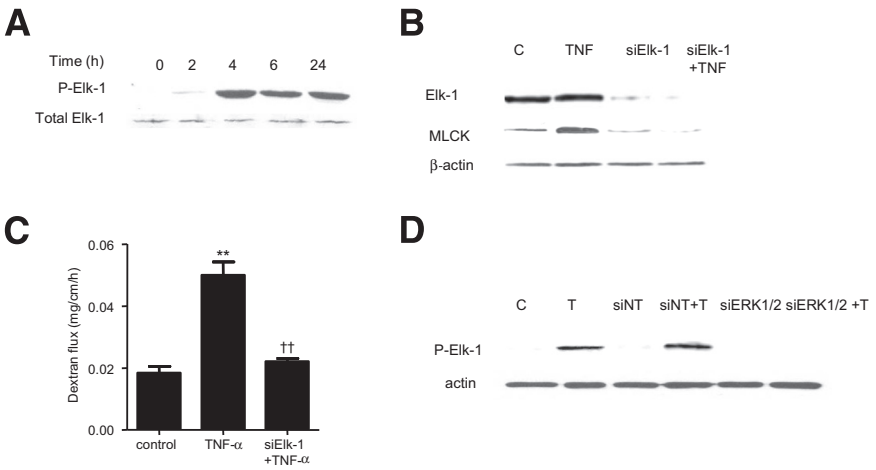


**Figure 11** **A**: TNF-α causes a time-dependent increase in Elk-1 phosphorylation; total ERK1/2 was used for equal protein loading. **B**: Elk-1 siRNA transfection results in a near-complete depletion of mouse intestinal Elk-1 protein expression and prevents the TNF-α–induced increase in mouse intestinal MLCK protein expression. **C**: Elk-1 silencing inhibits the TNF-α–induced increase in mucosal-to-serosal flux of dextran 10K. **D**: siRNA-induced knockdown of ERK1/2 prevents TNF-α–induced phosphorylation of Elk-1 in mouse intestinal tissue. Data are expressed as means ± SEM. $n = 3$. Experimental period, 24 hours (**B** and **C**); 4 hours (**D**). $^{**}P < 0.0001$ versus control. $^{††}P < 0.0001$ versus TNF-α treatment.

activity was responsible for the TNF-α–induced increase in Caco-2 TJ permeability. Presumably, the increase in MLCK activity leads to myosin light chain phosphorylation and myosin-$Mg^{2+}$-ATPase–dependent opening of the intestinal TJ barrier.[42]

As for the molecular mechanisms that regulate the *MLCK* gene activation and gene transcription, our studies suggest that the nuclear transcription factor Elk-1 is an important mediator of *MLCK* gene activity and Caco-2 TJ permeability. Elk-1 belongs to the ETS domain transcription factor family and the ternary complex factor subfamily and is a direct substrate of ERK1/2.[34,43–45] On activation, Elk-1 forms a ternary complex with the serum response factor protein and binds to the serum response element, inducing activation of the target gene.[34] Serine phosphorylation of Elk-1 (Ser383 and Ser389) is necessary for the transcriptional regulation. ERK1/2 is known to induce phosphorylation and activation of Elk-1.[33,34,46] Our present results show that TNF-α causes ERK1/2-dependent phosphorylation and activation of Elk-1. Moreover, inhibition of ERK1/2 activation or ERK1/2 knockdown prevented TNF-α activation of Elk-1, suggesting that Elk-1 activation is directly regulated by ERK1/2. Our results also showed that Elk-1 plays an essential role in TNF-α up-regulation of *MLCK*, and siRNA silencing of Elk-1 inhibited the increase in *MLCK* gene activity and mRNA transcription and also inhibited the increase in Caco-2 TJ permeability. Our promoter binding studies demonstrated binding of activated Elk-1 to the putative binding site (serum response element) on the *MLCK* promoter region, and site-directed mutagenesis studies confirmed the requirement of the serum response element in TNF-α up-regulation of the promoter activity. Thus, our data suggest that binding of activated Elk-1 to the serum response element is important in the regulation of *MLCK* promoter activity. Taken together, our findings suggest that the ERK1/2 activation of Elk-1 leads to *MLCK* promoter activation and subsequent increase in MLCK mRNA transcription and translation and MLCK-dependent opening of the Caco-2 TJ barrier.

We also examined the *in vivo* mechanisms of TNF-α regulation of intestinal permeability, using recycling intestinal perfusion of isolated segment of mouse small intestine *in vivo*. In previous studies, intraperitoneal administration of TNF-α resulted in an increase in intestinal permeability to dextran 10K.[31] In the present studies, the increase in mouse intestinal permeability was associated with an increase in ERK1/2 activity, and intestinal tissue–specific silencing of ERK1/2 completely inhibited the TNF-α–induced increase in mouse intestinal permeability, suggesting that the TNF-α–induced increase in intestinal permeability is regulated by the ERK1/2 signaling pathway. Our *in vivo* studies also indicated that TNF-α causes an ERK1/2-dependent activation of Elk-1 and that Elk-1 activation was required for the TNF-α–induced increase in intestinal MLCK expression and intestinal permeability. These data suggest that a similar signaling mechanism regulates the effect of TNF-α on intestinal permeability both *in vivo* and *in vitro*. Our studies also suggest that *in vivo* targeting of ERK1/2 signaling pathways is effective in preventing the TNF-α–induced increase in intestinal permeability. To our knowledge, this is the first study to show that the *in vivo* activation of the ERK1/2 signaling pathway regulates the TNF-α–induced increase in intestinal permeability.

In conclusion, our results provide new insight into the intracellular signaling pathways and molecular processes that regulate TNF-α modulation of intestinal TJ permeability. The findings suggest that TNF-α causes a rapid activation of ERK1/2, which in turn leads to phosphorylation and activation of Elk-1; the activated Elk-1 binds to the serum response element on the *MLCK* promoter, leading to *MLCK* gene activation, transcription, protein expression, and MLCK-dependent opening of the intestinal TJ barrier. Our *in vivo* studies also demonstrated the feasibility of therapeutic targeting of ERK1/2 and Elk-1 to prevent the TNF-α–induced increase in intestinal TJ permeability *in vivo*.

## Supplemental Data

Supplemental material for this article can be found at *http://dx.doi.org/10.1016/j.ajpath.2013.09.001*.

## References


1. Arrieta MC, Madsen K, Doyle J, Meddings J: Reducing small intestinal permeability attenuates colitis in the IL10 gene-deficient mouse. Gut 2009, 58:41–48
2. Hollander D: Intestinal permeability, leaky gut, and intestinal disorders. Curr Gastroenterol Rep 1999, 1:410–416
3. Turner JR: Intestinal mucosal barrier function in health and disease. Nat Rev Immunol 2009, 9:799–809
4. Hollander D: Crohn's disease—a permeability disorder of the tight junction? Gut 1988, 29:1621–1624
5. Ma TY, Anderson JM, Turner JR: Tight junctions and the intestinal barrier. Edited by Johnson LR, Ghishan FK, Kaunitz JD, Merchant JL, Said HM, Wood JDs. Physiology of the Gastrointestinal Tract. ed 5. Waltham, MA, Academic Press, 2012, pp 1043–1088
6. Ma TY, Boivin MA, Ye D, Pedram A, Said HM: Mechanism of TNF-{alpha} modulation of Caco-2 intestinal epithelial tight junction barrier: role of myosin light-chain kinase protein expression. Am J Physiol Gastrointest Liver Physiol 2005, 288:G422–G430
7. Suenaert P, Bulteel V, Lemmens L, Noman M, Geypens B, Van Assche G, Geboes K, Ceuppens JL, Rutgeerts P: Anti-tumor necrosis factor treatment restores the gut barrier in Crohn's disease. Am J Gastroenterol 2002, 97:2000–2004
8. Breese EJ, Michie CA, Nicholls SW, Murch SH, Williams CB, Domizio P, Walker-Smith JA, MacDonald TT: Tumor necrosis factor alpha-producing cells in the intestinal mucosa of children with inflammatory bowel disease. Gastroenterology 1994, 106:1455–1466
9. Reinecker HC, Steffen M, Witthoeft T, Pflueger I, Schreiber S, MacDermott RP, Raedler A: Enhanced secretion of tumour necrosis factor-alpha, IL-6, and IL-1 beta by isolated lamina propria mononuclear cells from patients with ulcerative colitis and Crohn's disease. Clin Exp Immunol 1993, 94:174–181
10. Watson AJ, Duckworth CA, Guan Y, Montrose MH: Mechanisms of epithelial cell shedding in the mammalian intestine and maintenance of barrier function. Ann N Y Acad Sci 2009, 1165:135–142
11. Worrall NK, Chang K, LeJeune WS, Misko TP, Sullivan PM, Ferguson TB Jr., Williamson JR: TNF-alpha causes reversible in vivo systemic vascular barrier dysfunction via NO-dependent and -independent mechanisms. Am J Physiol 1997, 273:H2565–H2574
12. Caty MG, Guice KS, Oldham KT, Remick DG, Kunkel SI: Evidence for tumor necrosis factor-induced pulmonary microvascular injury after intestinal ischemia-reperfusion injury. Ann Surg 1990, 212:694–700
13. Turner JR: Molecular basis of epithelial barrier regulation: from basic mechanisms to clinical application. Am J Pathol 2006, 169: 1901–1909
14. Rodriguez P, Darmon N, Chappuis P, Candalh C, Blaton MA, Bouchaud C, Heyman M: Intestinal paracellular permeability during malnutrition in guinea pigs: effect of high dietary zinc. Gut 1996, 39: 416–422
15. Clayburgh DR, Musch MW, Leitges M, Fu YX, Turner JR: Coordinated epithelial NHE3 inhibition and barrier dysfunction are required for TNF-mediated diarrhea in vivo. J Clin Invest 2006, 116: 2682–2694
16. Ma TY, Iwamoto GK, Hoa NT, Akotia V, Pedram A, Boivin MA, Said HM: TNF-alpha-induced increase in intestinal epithelial tight junction permeability requires NF-kappa B activation. Am J Physiol Gastrointest Liver Physiol 2004, 286:G367–G376
17. Turner JR, Angle JM, Black ED, Joyal JL, Sacks DB, Madara JL: PKC-dependent regulation of transepithelial resistance: roles of MLC and MLC kinase. Am J Physiol 1999, 277:C554–C562
18. Turner JR, Rill BK, Carlson SL, Carnes D, Kerner R, Mrsny RJ, Madara JL: Physiological regulation of epithelial tight junctions is associated with myosin light-chain phosphorylation. Am J Physiol 1997, 273:C1378–C1385
19. Ye D, Ma I, Ma TY: Molecular mechanism of tumor necrosis factor-alpha modulation of intestinal epithelial tight junction barrier. Am J Physiol Gastrointest Liver Physiol 2006, 290:G496–G504
20. Liu X, Xu J, Mei Q, Han L, Huang J: Myosin light chain kinase inhibitor inhibits dextran sulfate sodium-induced colitis in mice. Dig Dis Sci 2013, 58:107–114
21. Moriez R, Salvador-Cartier C, Theodorou V, Fioramonti J, Eutamene H, Bueno L: Myosin light chain kinase is involved in lipopolysaccharide-induced disruption of colonic epithelial barrier and bacterial translocation in rats. Am J Pathol 2005, 167:1071–1079
22. Ieda Y, Waguri-Nagaya Y, Iwahasi T, Otsuka T, Matsui N, Namba M, Asai K, Kato T: IL-1beta-induced expression of matrix metalloproteinases and gliostatin/platelet-derived endothelial cell growth factor (GLS/PD-ECGF) in a chondrosarcoma cell line (OUMS-27). Rheumatol Int 2001, 21:45–52
23. Fyfe M, Bergström M, Aspengren S, Peterson A: PAR-2 activation in intestinal epithelial cells potentiates interleukin-1beta-induced chemokine secretion via MAP kinase signaling pathways. Cytokine 2005, 31: 358–367
24. Hide I: [Mechanism of production and release of tumor necrosis factor implicated in inflammatory diseases]. Japanese. Nihon Yakurigaku Zasshi 2003, 121:163–173
25. Kyriakis JM, Avruch J: Protein kinase cascades activated by stress and inflammatory cytokines. Bioessays 1996, 18:567–577
26. Al-Sadi RM, Ma TY: IL-1beta causes an increase in intestinal epithelial tight junction permeability. J Immunol 2007, 178: 4641–4649
27. Clayburgh DR, Rosen S, Witkowski ED, Wang F, Blair S, Dudek S, Garcia JG, Alverdy JC, Turner JR: A differentiation-dependent splice variant of myosin light chain kinase, MLCK1, regulates epithelial tight junction permeability. J Biol Chem 2004, 279:55506–55513
28. Al-Sadi R, Ye D, Dokladny K, Ma TY: Mechanism of IL-1beta-induced increase in intestinal epithelial tight junction permeability. J Immunol 2008, 180:5653–5661
29. Al-Sadi R, Guo S, Dokladny K, Smith MA, Ye D, Kaza A, Watterson DM, Ma TY: Mechanism of interleukin-1beta induced-increase in mouse intestinal permeability in vivo. J Interferon Cytokine Res 2012, 32:474–484
30. Clayburgh DR, Barrett TA, Tang Y, Meddings JB, Van Eldik LJ, Watterson DM, Clarke LL, Mrsny RJ, Turner JR: Epithelial myosin light chain kinase-dependent barrier dysfunction mediates T cell activation-induced diarrhea in vivo. J Clin Invest 2005, 115: 2702–2715
31. Ye D, Guo S, Al-Sadi R, Ma TY: MicroRNA regulation of intestinal epithelial tight junction permeability. Gastroenterology 2011, 141: 1323–1333
32. Babu GJ, Lalli MJ, Sussman MA, Sadoshima J, Periasamy M: Phosphorylation of Elk-1 by MEK/ERK pathway is necessary for c-Fos gene activation during cardiac myocyte hypertrophy. J Mol Cell Cardiol 2000, 32:1447–1457
33. Whitmarsh AJ, Shore P, Sharrocks AD, Davis RJ: Integration of MAP kinase signal transduction pathways at the serum response element. Science 1995, 269:403–407
34. Gille H, Kortenjann M, Thomae O, Moomaw C, Slaughter C, Cobb MH, Shaw PE: ERK phosphorylation potentiates Elk-1-mediated ternary complex formation and transactivation. EMBO J 1995, 14: 951–962
35. Zhang L, Zhu H, Davis JJ, Jacob D, Wu S, Teraishi F, Gutierrez A, Wang Y, Fang B: Lack of p38 MAP kinase activation in TRAIL-resistant cells is not related to the resistance to TRAIL-mediated cell death. Cancer Biol Ther 2004, 3:296–301
36. Al-Sadi R, Guo S, Ye D, Dokladny K, Alhmoud T, Ereifej L, Said HM, Ma TY: Mechanism of IL-1beta modulation of intestinal

epithelial barrier involves p38 kinase and activating transcription factor-2 activation. J Immunol 2013, 190:6596–6606
37. Al-Sadi R, Ye D, Said HM, Ma TY: Cellular and molecular mechanism of interleukin-1beta modulation of CACO-2 intestinal epithelial tight junction barrier. J Cell Mol Med 2011, 15:970–982
38. Dai J, Rabie AB: VEGF: an essential mediator of both angiogenesis and endochondral ossification. J Dent Res 2007, 86:937–950
39. Dai C, Zhao DH, Jiang M: VSL#3 probiotics regulate the intestinal epithelial barrier in vivo and in vitro via the p38 and ERK signaling pathways. Int J Mol Med 2012, 29:202–208
40. Yang R, Harada T, Li J, Uchiyama T, Han Y, Englert JA, Fink MP: Bile modulates intestinal epithelial barrier function via an extracellular signal related kinase 1/2 dependent mechanism. Intensive Care Med 2005, 31:709–717
41. Pinton P, Braicu C, Nougayrede JP, Laffitte J, Taranu I, Oswald IP: Deoxynivalenol impairs porcine intestinal barrier function and decreases the protein expression of claudin-4 through a mitogen-activated protein kinase-dependent mechanism. J Nutr 2010, 140: 1956–1962
42. Ma TY, Hoa NT, Tran DD, Bui V, Pedram A, Mills S, Merryfield M: Cytochalasin B modulation of Caco-2 tight junction barrier: role of myosin light chain kinase. Am J Physiol Gastrointest Liver Physiol 2000, 279:G875–G885
43. Uhlig U, Haitsma JJ, Goldmann T, Poelma DL, Lachmann B, Uhlig S: Ventilation-induced activation of the mitogen-activated protein kinase pathway. Eur Respir J 2002, 20:946–956
44. Deora AA, Hajjar DP, Lander HM: Recruitment and activation of Raf-1 kinase by nitric oxide-activated Ras. Biochemistry 2000, 39:9901–9908
45. Sharrocks AD: Complexities in ETS-domain transcription factor function and regulation: lessons from the TCF (ternary complex factor) subfamily. The Colworth Medal Lecture. Biochem Soc Trans 2002, 30:1–9
46. Price MA, Cruzalegui FH, Treisman R: The p38 and ERK MAP kinase pathways cooperate to activate ternary complex factors and c-Fos transcription in response to UV light. EMBO J 1996, 15:6552–6563